



## Photon energy limits for food irradiation: a feasibility study

J. Mckeown<sup>a, \*</sup>, L. Armstrong<sup>a</sup>, M.R. Cleland<sup>a</sup>, N.H. Drewell<sup>a</sup>, J. Dubeau<sup>b</sup>,  
C.B. Lawrence<sup>a</sup>, D. Smyth<sup>a</sup>

<sup>a</sup>AECL Accelerators, 10 Hearst Way, Kanata, Ont., Canada K2L 2P4

<sup>b</sup>Detec, 920 Chemin Cook, Aylmer, Que., Canada J9H 5C9

Received 13 June 1997; received in revised form 27 October 1997

---

### Abstract

The penetrating nature of the photons produced by the X-ray (bremsstrahlung) process makes them attractive for the treatment of dense materials in industrial radiation processing. The inefficiency of the conversion process can be balanced by the exposure of high  $Z$  materials to electrons with high energy. However, activation of the product being irradiated and the equipment imposes energy limits. Results of a theoretical and experimental study to investigate the key parameters have resulted in recommendations for the design of X-ray converters in the electron energy range 7 to 11 MeV. Results of the Monte Carlo calculations and the methods used in conversion experiments with the 50 kW IMPELA accelerator are reported. © 1998 Elsevier Science Ltd. All rights reserved.

*Keywords:* Food irradiation; Bremsstrahlung; X-ray; Activation; Electron energy

---

### 1. Introduction

When the irradiation of food becomes commercial on a large scale, new radiation sources will be needed. <sup>60</sup>Co supply will be inadequate (Mylvaganam and Ronchika, 1990) and the photons from the developed large radioactive sources will not provide the required penetration for commercial throughput of some high density products (Cleland et al., 1990). Electron accelerators with high power X-ray (bremsstrahlung) converters already in service at 5 MeV (Sato et al., 1993) have been suggested as satisfying the market need. A major drawback of this technology is the low efficiency of the X-ray conversion process and suggestions have been made to increase the efficiency by raising the electron energy.

There are two major concerns in raising the electron energy. The electron energy is limited by the onset of nuclear reactions in the processing equipment and in

the irradiated material. These concerns are compounded by the use of high atomic number targets to increase the photon yield. The issues were well understood by early researchers in the field (Becker, 1983) leading to the adoption by the World Health Organization of a 5 MeV limit (WHO Report, 1981). More recent work has indicated that this limit is unnecessarily conservative and a recent experts' committee of the International Atomic Energy Agency has made a recommendation to allow energies up to 7.5 MeV to be used (Brynjolfsson, 1995).

A component part of the recommendation is that experiments be undertaken to confront the key issues with modern accelerators and diagnostic equipment, leading to a quantification of the processes involved. The objective of the work reported here is to make a first step in examining the feasibility of using high atomic number X-ray converters over the energy range 7 to 11 MeV. In this work, we take advantage of the availability of the 50 kW IMPELA accelerator in a laboratory environment at Chalk River, where high resolution spectrometers are available to assist in the

---

\* Corresponding author.

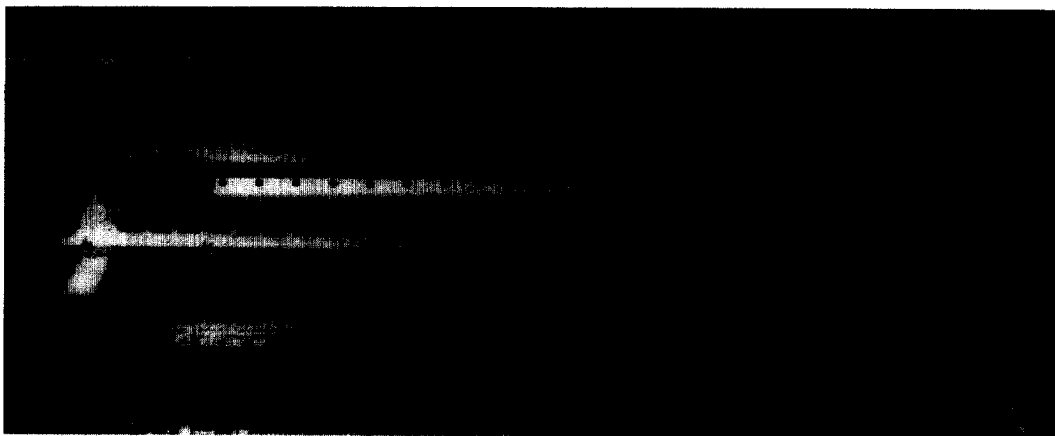


Fig. 1. Photograph of the X-ray converter on the IMPELA accelerator.

understanding and in the identification of the processes involved.

## 2. Method

The IMPELA accelerator (Ungrin, 1988; McKeown et al., 1995) at Chalk River operates at 0 to 50 kW over the energy range 6 to 12 MeV. It can be configured to meet the needs of experimenters wishing to characterize beam parameters for radiation processing (McKeown and Jones, 1987).

Two X-ray converters were built. Tantalum and stainless steel were chosen as a compromise between photon yield, residual radioactivity, mechanical properties, fabrication cost and operational simplicity for a commercial environment. The tantalum converter was designed to maximize photon yield and provide sufficient cooling in four independent channels to handle a beam power of 100 kW over 80 cm of the one dimensional scan of the electron beam. The maximum temperature on the tantalum surface was designed to be 350°C. The 1.5 mm thick curved tantalum sheet is backed with two 2.5 mm thick cooling channels and 8 mm of aluminum. The total thickness is sufficient to stop a primary 11 MeV electron beam. A photograph of the converter mounted 10 cm outside the titanium window of the horizontally oriented accelerator is shown in Fig. 1.

The stainless steel converter was similar in radiation design except that cooling was not segmented but rather formed a single 80 × 3.2 mm channel behind the 3.2 mm thick converter plate. The backing plate was stainless steel. The converter was run at 50 kW output power from the accelerator (Fig. 2).

X-ray profiles were measured at a distance 35 cm from the converter with an aluminum phantom and FWT dosimetry film. The film was placed at a depth

of 0.9 cm in the aluminum. Although space did not permit the use of a phantom large enough to give full scatter conditions, an error of 10% in the measurement of the full width at half maximum of the tantalum X-ray beam of 20 cm is thought to be adequate in comparison with other uncertainties. Neutron measurements were made with bubble detectors. These detectors are threshold detectors with a flat response above 200 keV. Several of the detectors were used to measure the neutron fields inside and outside the concrete shield. Their high sensitivity precluded direct measurements near the target and indirect measurements were made by exposing aluminium samples 5 × 5 × 0.1 cm for 5 min. A count rate of 200,000 count/min from these samples indicated that near the tantalum target the neutron flux was 10<sup>7</sup> neutrons/cm<sup>2</sup>.s at 10 MeV. About 8 m from the target, the neutron flux, as measured with the bubble detectors, was 5 times greater with the tantalum than with the stainless steel at 10 MeV.

The gamma spectrometer used to measure the induced activity was an ORTEC Gem 15180 high purity Ge(Li) coaxial detector feeding into an Aptec NIM 6300 linear amplifier. A multi-channel analyzer, Aptec 3004 MCA with built in 900 ns ADC collected the data. AECL customized software was used to identify the peaks and attribute them to specific iso-

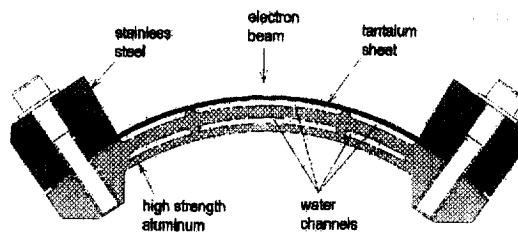


Fig. 2. Cross section of tantalum converter.

topes including the annihilation peaks coming from the positrons created by the high energy gamma photons following the decay of <sup>24</sup>Na and <sup>38</sup>Cl.

The Monte Carlo codes are described by Halbleib et al. (1992) and Briesmeister (1993). The geometry for each case was set up by Detec (Detec, 1997) and the code executed on a set of Pentium personal computers. Experimental conditions dictated the scope of the work and the challenge was to compare depth-dose measurements with electron-photon transport results and the activation with the neutron transport results for these conditions. The characteristics of the neutron generation were derived by hand from published cross-sections.

### 3. Results from calculations and experiments

#### 3.1. Throughput

Expectations of higher photon yield with increased atomic number and incident electron energy are based on the interaction processes summarized in Fig. 3, reproduced from the theoretical work of Lone (Lone, 1989).

The mass radiative stopping power,  $(S/\rho)_{\text{rad}}$ , describing the rate of bremsstrahlung production in a material with atomic number,  $Z$ , by electrons of energy,  $T$ , is proportional to:

$$(S/\rho)_{\text{rad}} \propto (N_A Z^2/A)T$$

The photon radiation yield,  $\gamma$ , of the electron is the total fraction of the initial energy,  $T$ , that is emitted as electromagnetic radiation while the electron slows and comes to rest. It can be defined as:

$$\gamma(T, Z) = (S/\rho)_{\text{rad}} / [(S/\rho)_{\text{col}} + (S/\rho)_{\text{rad}}]$$

Fig. 3 shows the mass stopping power,  $(S/\rho)_{\text{col}}$  and  $(S/\rho)_{\text{rad}}$ , for collision and radiation losses, respectively, as a function of atomic number,  $Z$ , and for the given values of electron energy,  $T$ . For tantalum, the Monte Carlo calculations predicted an efficiency (the fraction of kinetic energy converted to photons in thick targets) of 20, 24.6, 28.6 and 30% at 5, 7, 9 and 10 MeV respectively. In practice, for  $4\pi$  emission, a smaller fraction actually escapes the tantalum converter: 12% (5 MeV), 17% (7 MeV), 21.5% (9 MeV) and 23% (10 MeV). The fraction that escapes in the forward direction is even less, 19.3% at 10 MeV. When 5 mm of cooling water and an 8 mm electron absorber are introduced into the model, the 10 MeV value drops to 18.6%. These results agree well with a previous measurement of 20% at 10 MeV (McKeown and Sherman, 1985).

In the IMPELA system the electron beam scans  $\pm 15^\circ$  with respect to the center while the product is translating at slow speed perpendicular to the scan direction. We chose to model the irradiation of a product that consists of an 80 cm cube of water in a single pass to obtain the base data from which a multi-pass system of any number of passes can be derived. The effect of product motion 15 cm from the converter was included in the calculation. Depth-dose curves were tallied down the center of the cube.

A multi-pass system consisting of  $80 \times 80 \times 20$  cm slabs of water, piled three deep, yielded a capture efficiency of 94%. Shuffling of the slabs achieved max/min ratios of 1.33 for tantalum and 1.22 for stainless steel. The procedure was to rotate the front product slab and move it to the back position in each of 3 passes. Hence each slab is irradiated through one side for the most intense pass and then irradiated through the other face for the two low intensity passes. Results in Fig. 4 show that throughput increases almost linearly with energy as expected from previous studies. The throughput from a stainless steel converter at 7.5 MeV is about the same as tantalum at 5 MeV while at 10 MeV the stainless steel throughput is greater than tantalum at the existing energy limit of 5 MeV. A shift length of 12 h was chosen to provide a practical meaning to the results. Agreement between experiment and calculation was better than 10% for a scanned beam and the improvised conveyor system.

Photon yield emerging from the converter is also a strong function of converter thickness and any assessment of throughput must take this into account. Two energies were chosen. A 5 MeV limit is assumed for dc accelerators and an 8.5 MeV limit is chosen for radio-frequency accelerators because of the risks of activation. This limit is indicated by the physics, although

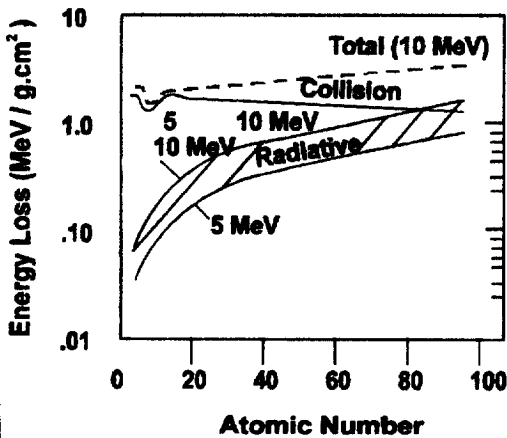


Fig. 3. Interaction processes of electrons with matter. At 10 MeV, the probability of producing a photon equals the probability of an electron collision.

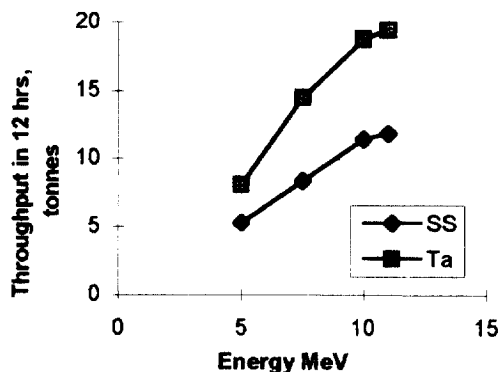


Fig. 4. Throughput versus energy for two converters. The data assumes 50 kW beam for a dose of 10 kGy.

regulators are likely to choose a value with a safety margin as indicated in the IAEA report. Depth-dose profiles averaged over the first 20 cm for different tantalum converter thicknesses were calculated at these two energies. The results are presented in Fig. 5.

### 3.2. Activation

Activation arises from the absorption of neutrons primarily created in the tantalum target and from direct photon interaction. When operated above the ( $\gamma, n$ ) threshold of the X-ray converter, two radioactive nuclei,  $^{180}\text{Ta}$  and  $^{182}\text{Ta}$  are formed respectively by ( $\gamma, n$ ) and ( $n, \gamma$ ) reactions on the naturally abundant  $^{181}\text{Ta}$ . The former has an 8.1 h half-life and the mostly-beta saturation activity of  $1.6 \times 10^9 \text{ Bq/cm}^2$  is easily shielded. The latter, with a half-life of 114 days and emitting a 1.2 MeV gamma ray, has a projected saturation activity of  $4 \times 10^6 \text{ Bq/cm}^2$  per 1% neutron capture and without shielding the projected exposure rate at 10 cm from the surface at center is 1 mGy/h per 1% neutron capture. In our experiments, we achieved saturation of the  $^{180}\text{Ta}$  only, with measured surface radiation fields of about one mGy/h immediately after shutdown. After several weeks of experimentation, the residual levels after allowing the  $^{180}\text{Ta}$  to decay were a few  $\mu\text{Gy/h}$ .

The topic of induced activity in the irradiated product has been examined previously with electron accelerators by Glass and Smith (1959)<sup>1</sup> and Koch and Eisenhower (1967) and most recently by Miller and Hedemann Jensen (1987). Most of these experiments concentrated on electron irradiation where high dose rates are possible. In our work, experiments were devised using X-ray converters for the processing of

<sup>1</sup> This report describes the first measurements on induced activity in meat irradiated with high energy electrons.

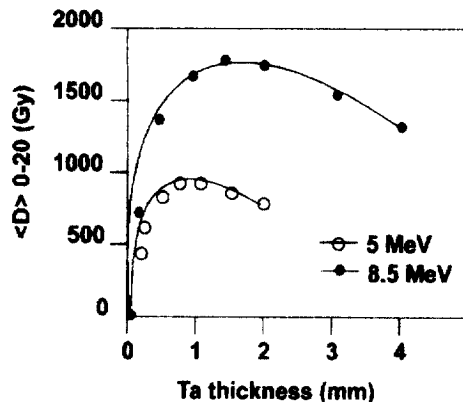


Fig. 5. Variation of the dose averaged over the first 20 cm of water (D-20) as a function of the thickness of the converter for 5 and 8.5 MeV electron beams.

food to assist engineering judgments concerning their practicality. Results from a first examination of the activation risks are shown in Fig. 6.

Neutrons are produced by direct interaction of the electrons with the target nucleus or through virtual photon interactions as described by Lone (1989). Fig. 6(left) shows the relative growth in neutron flux when the energy is increased. The neutron production rate from the tantalum target as measured with bubble detectors placed 8 m from the target is calculated to be  $0.9 \times 10^{11}$  neutrons/s for 10 MeV and  $2.1 \times 10^{11}$  neutrons/s for 11 MeV at 50 kW. Fig. 6(right) shows the count rate integrated over the hamburger surface as measured by a Geiger counter from a sample of red meat that was exposed to a dose of 10 kGy when placed at a distance of 14 cm from the converter. The threshold and relative shape of the two curves would seem to confirm the mechanisms that give rise to activation. However, identification of the active isotopes required the gamma spectrometer and the quantification of the processes were carried out by the Monte Carlo calculations. The neutron yield from stainless steel is more than two orders of magnitude lower and the formation of  $^{56}\text{Mn}$  in the target is the main practical consequence. The activation in the meat with the stainless steel converter is a direct effect on the nitrogen as discussed below.

Table 1 shows some of the principal isotopes in red meat that have nuclear properties that might be candidates for activation. The key elements are nitrogen, sodium and chlorine, the latter two arising from the concentrations of common salt. All are activated by neutron absorption except  $^{13}\text{N}$ , which is produced by direct photo-neutron interaction on nitrogen. Results of the activation of specific isotopes are shown in Table 2, as measured in the gamma spectrometer following the irradiation of red meat to a dose of 10 kGy

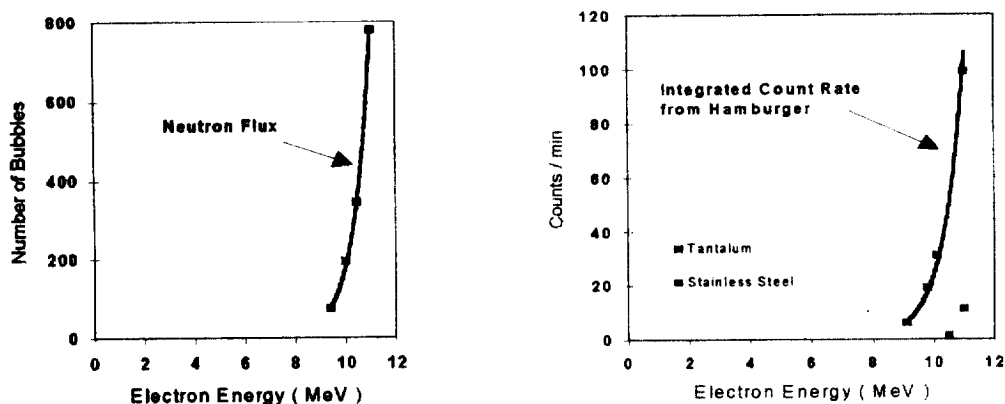


Fig. 6. Measured neutron production from tantalum converter and resultant activation of a red meat sample as a function of energy.

placed 14 cm from the two X-ray converters (tantalum and stainless steel). Two meat samples were chosen. The steak was cut from an unprocessed rump roast while the hamburger was selected for its claim that there were no additives or preservatives. Exposure at a rate of 100 Hz was for 100,000 accelerator pulses, using the 100 mA beam incident on the converter plate and counting began 10 min after completion of the irradiation. Data for the 10 MeV tantalum run on hamburger was unfortunately lost.

There was no difficulty identifying the particular nuclide. All gamma ray spectrum lines were within a few keV of known values and the half lives were as expected. Activities for 11 MeV were typically about an order of magnitude above background and for both steak and hamburger the  $^{13}\text{N}$  isotope dominates and disappears for both products below the  $(\gamma, n)$  threshold for  $^{14}\text{N}$ . The concentration of common salt as indicated by the amount of chlorine and sodium is much higher for hamburger than steak. Assuming that the neutrons were coming exclusively from the converter, theory suggests that the sodium and chlorine should

increase by a factor of 2.5 over this energy range. This compares with the experimentally measured value of 1.8. The  $^{38}\text{Cl}/^{24}\text{Na}$  ratio is in closer agreement between theory and experiment with values of 1.8 and 2.0, respectively. However, absolute calibrations involving yields and detector efficiency are in disagreement by a factor of 4.3.

#### 4. Discussion

As expected, the tantalum converter provides increased throughput over stainless steel for the same processing conditions. At 7.5 MeV the gain is 74%, while at 10 MeV the gain is 71%. At 10 MeV the X-ray yield from stainless steel is still 50% better than existing accelerator technologies using tantalum at 5 MeV. The high neutron generation with tantalum at 10 MeV is considered unacceptable for commercial operational conditions, especially as it can be eliminated at 7.5 MeV for a penalty of a reduced throughput of 24%. At this energy, a 7.5 MeV tantalum converter is

Table 1  
Concentrations and nuclear properties of isotopes capable of contributing to activation by direct transmutation or neutron absorption

Isotope	Food %	Thermal neutron capture cross-section (b)	$(\gamma, n)$ threshold (MeV)	Formed isotope half-life
$^1\text{H}$	59.86	0.33	—	—
$^2\text{H}$	0.01	0.0006	2.225	—
$^{12}\text{C}$	9.90	0.0037	18.72	—
$^{14}\text{N}$	0.95	1.88	10.55	9.9 m
$^{16}\text{O}$	29.15	$< 5 \cdot 10^{-6}$	15.67	—
$^{23}\text{Na}$	0.02	0.53	12.41	15.0 h
$^{31}\text{P}$	0.04	0.2	12.32	—
$^{35}\text{Cl}$	0.008	30	12.6	$10^5$ y
$^{37}\text{Cl}$	0.0026	0.56	10.3	37.5 m
$^{39}\text{K}$	0.06	1.89	13.1	$1.3 \times 10^9$ y

Table 2  
Activity in Bq/g of specific isotopes in steak and hamburger following irradiation by photons to 10 kGy

		Energy/nuclide (keV)					
		10 MeV			11 MeV		
		<sup>13</sup> N, 511	<sup>24</sup> Na, 2,753	<sup>38</sup> Cl, 2,167	<sup>13</sup> N, 511	<sup>24</sup> Na, 2,753	<sup>38</sup> Cl, 2,167
Hamburger	activity with Ta converter (Bq/g)	—	—	—	9.8	5.5	14.6
	activity with SS converter (Bq/g)	0.01	0.01	0.04	2.4	0.01	0.02
Steak	activity with Ta converter (Bq/g)	0.001	0.08	0.08	20.3	0.43	0.87

still better than a 10 MeV stainless steel converter by 31%. The stainless steel converter carries an additional hazard at 10 MeV as the photon spectrum is harder and photons are present with energies greater than the photo-neutron threshold of many isotopes. For a food product with a high proportion of nitrogen, an error of 10% in the energy calibration could lead to activation suggesting a need for on-line energy monitoring.

First simulation results considered photo-neutrons which originate from the tantalum converter only. The activation of food can also arise from the <sup>2</sup>H ( $\gamma, n$ ) reaction (threshold of 2.25 MeV) as deuterium exists at a concentration of 0.015% in the hydrogen present. Hence, the water channels and the food itself are neutron sources. Our simulations showed that for a 10 MeV electron beam, each cooling channel contributes 0.05% of the tantalum contribution, while the food itself contributes 0.15% to a 2.5 cm slice of steak. This contribution is small but it is intrinsic. Over 90% of the neutrons escape in this geometry and of those absorbed, hydrogen captures 98%, <sup>35</sup>Cl and <sup>37</sup>Cl capture 1.69%, <sup>23</sup>Na captures 0.06% and <sup>2</sup>H captures  $3 \times 10^{-3}$ %. We verified that these numbers are independent of product volume; thus  $2.6 \times 10^{-2}$  Bq/g of <sup>38</sup>Cl and  $1.5 \times 10^{-2}$  Bq/g of <sup>24</sup>Na are due to neutrons created within the food at a dose of 10 kGy at 10 MeV. They should be compared with the natural background radioactivity in food which for <sup>40</sup>K is typically 0.15 Bq/g.

For a practical geometry designed to optimize throughput, one may expect increased activation due to deuterium. A larger product mass increases the net number of neutrons produced and it also results in a larger neutron moderator which enhances capture. One must also expect a peak in the activation as a greater product mass leads to an increase in the attenuation of the X-rays and a deficit in photo-neutron generation as the depth is increased. Our simulations confirmed these expectations with a peak near 0.23 Bq/g of <sup>38</sup>Cl and 0.13 Bq/g of <sup>24</sup>Na for a 10 MeV electron beam and a dose of 10 kGy.

The measuring techniques did not permit a test at the expert committee's suggestion of an incident elec-

tron energy limit of 7.5 MeV. Also, irradiation times with photons do not easily allow the standard technique used in electron irradiations of using high doses to excite the events of low probability. Our work at higher energy shows that activation products observed in food are consistent with our understanding of the mechanisms involved and the known thresholds for neutron production and direct interactions. Such knowledge should assist regulators in making judgments of acceptable energy limits where detection is impractical.

## 5. Summary

An investigation of the energy limits for photon irradiation of food has led to an appraisal of the key parameters needed in the design and construction of a practical food irradiator. We conclude that no material will be acceptable at 11 MeV or above if detectable activity from <sup>13</sup>N is to be avoided. Tantalum is not an acceptable material at 10 MeV or above because of contamination of the processing equipment and the product. Our work shows that stainless steel is acceptable at 10 MeV although there remains a penalty in the throughput of 21% over tantalum at 7.5 MeV. The stainless steel throughput at 10 MeV is better than existing technologies at 5 MeV, although this choice should only be made with an accelerator having good energy control. We conclude that tantalum is a good choice for the X-ray conversion material at 7.5 MeV with an advantage in conversion efficiency of 74% over stainless steel at 7.5 MeV and 50% over tantalum at 5 MeV and without risk of producing detectable activity in the processing equipment or the product.

## Acknowledgements

Grateful acknowledgment is given to T.J. Kunkel and S.T. Craig for operating the gamma spectrometer and to W. Mellors for the design of the tantalum converter.

## References

- Becker, R.L., 1983. In: Elias, P.S., Cohen, A.J. (Eds.), *Recent Advances in Food Irradiation*. Elsevier Biomedical Press, p. 285.
- Briesmeister, J.F., 1993. MNCP: a general Monte Carlo *N*-Particle Transport Code, Version 4-A, LA-12625-M.
- Brynjolfsson, A., 1995. Chairman Fa0/IAEA Consultants' Meeting on the Development of X-ray Machines for Food Irradiation.
- Cleland, M.R. et al., 1990. Advances in X-ray processing technology. *Radiat. Phys. Chem.* 35 (4–6), 632–637.
- DETEC Corporation, 1995–1997. J. Dubeau President. Reports done under contract to AECL Accelerators.
- Glass, R.A. and Smith, H.D., 1959. Radioactivities Produced in Foods by High-Energy Electrons. Stanford Research Institute Report S-572, No. 10 (DA 19-129-QM-1100).
- Halbleib, J.A. et al., 1992. ITS Version 3.0: The Integrated Tiger Series of Coupled Electron–Photon Monte Carlo Transport Codes. SAND91-1634.
- Koch, H.W., Eisenhower, E.H., 1967. Radioactivity criteria for radiation processing of foods. In: *Radiation Preservation of Foods*, Advances in Chemistry, Series 65. American Chemical Society, Washington, DC, pp. 87–108.
- Lone, M.A., 1989. Activation products in radiation processed meat. Atomic Energy of Canada Limited Report AECL-9959, p. 213.
- McKeown, J., Sherman, N.K., 1985. Linac based irradiators. *Radiat. Phys. Chem.* 25 (13), 103–109.
- McKeown, J. et al., 1995. US Patent No. 5,401,973.
- McKeown, J., Jones, R.T., 1987. Important aspects of linac beams for food irradiation. *Nucl. Instrum. Methods B* 24–25, 976–981.
- Miller, A., Hedemann Jensen, P., 1987. Measurements of induced radioactivity in electron- and photon-irradiated beef. *Appl. Radiat. Isot.* 38 (7), 507–512.
- Mylvaganam, C.K., Ronchika, R.A., 1990. *Radiat. Phys. Chem.* 35 (4–6), 602–605.
- Sato, Y. et al., 1993. Sterilization of X-ray products by 5 MeV bremsstrahlung. *Radiat. Phys. Chem.* 42 (4–6), 621–624.
- Ungrin, J., 1988. IMPELA Group Proc. Eur Part. Acc. Conf. EPAC, pp. 1515.
- WHO Joint Report of FAO/IAEA/WHO Expert Committee on the Wholesomeness of Irradiated Food, 1981. WHO Technical Report, Series #659.